


RESEARCH ARTICLE



SIRT1 promotes the progression and chemoresistance of colorectal cancer through the p53/miR-101/KPNA3 axis

Xiao-Wei Wang, Ying-Hao Jiang, Wei Ye, Chun-Fa Shao, Jian-Jin Xie, and Xia Li 

Department of Anorectal Surgery, The First People's Hospital of Wenling, Wenling, China

ABSTRACT

Introduction: Sirtuin 1 (SIRT1) is a key modulator in several types of cancer, including colorectal cancer (CRC). Here, we probed into the molecular mechanism of SIRT1 regulating the development and chemoresistance of CRC.

Methods: Differentially expressed genes related to the growth, metastasis and chemoresistance of CRC were identified by bioinformatics analysis. The expression of SIRT1 in clinical tissues from CRC patients and CRC cell lines was detected by RT-qPCR. Interactions among SIRT1, p53, miR-101 and KPNA3 were analyzed. The effect of SIRT1 on the cell viability, migration, invasion, epithelial-mesenchymal transformation and chemoresistance to 5-FU was evaluated using loss-function investigations in CRC cells. Finally, a xenograft model of CRC and a metastasis model were constructed for further exploration of the roles of SIRT1 in vivo.

Results: SIRT1 was elevated in CRC tissues and cell lines. SIRT1 decreased p53 via deacetylation, and consequently downregulated the expression of miR-101 while increasing that of the miR-101 target gene KPNA3. By this mechanism, SIRT1 enhanced the proliferation, migration, invasion, epithelial-mesenchymal transformation, and resistance to 5-FU of CRC cells. In addition, in vivo data also showed that SIRT1 promoted the growth, metastasis and chemoresistance to 5-FU of CRC cells via regulation of the p53/miR-101/KPNA3 axis.

Conclusions: In conclusion, SIRT1 can function as an oncogene in CRC by accelerating the growth, metastasis and chemoresistance to 5-FU of CRC cells through the p53/miR-101/KPNA3 axis.

ARTICLE HISTORY

Received 20 January 2022
Revised 29 June 2023
Accepted 30 June 2023

KEYWORDS

colorectal cancer; chemoresistance; SIRT1; p53; miR-101; KPNA3; metastasis; epithelial-mesenchymal transformation

Introduction

Colorectal cancer (CRC) represents the third most universal cancer, with over 90% of new sufferers in adults aged 50 y and older.^{1,2} As a heterogeneous disease, CRC often results from the combined effects of genetic and environmental factors³. Chemo-radiotherapy can be the standard of care for locally advanced CRC while the mortality rate of this cancer remains high due to several factors, such as treatment resistance and metastasis to distant organs.⁴⁻⁶ Therefore, innovative biomarker for CRC chemoresistance is necessitated.



SIRT1 participates in multiple biological processes and affects the development of several cancers, including CRC.^{7,8} SIRT1 expression is of clinical significance in CRC due to its significant association with the depth of tumor invasion, differentiation and tumor size, as well as metastasis.⁹ Moreover, promotion of the SIRT1-mediated autophagy has been indicated to induce CRC resistance to 5-fluorouracil (5-Fu), one of the most effective drugs and is widely used in treating CRC.^{10,11} SIRT1 overexpression can dramatically decrease acetylation of p53, a tumor suppressor that is critical for cancer survival and apoptosis; inhibition of the growth of CRC cells is modulated by the SIRT1/p53 axis.^{12,13} Notably, the p53/miR-101 circuit serves as a novel target for cancer therapy.¹⁴ microRNAs (miRNAs or miRs) function as a regulator in


CRC via their corresponding targets.¹⁵ A previous report by Jiang et al. has demonstrated that miR-101 is downregulated in CRC tissues, suggesting a promising therapeutic strategy for metastatic CRC.¹⁶ In addition, microarray analysis in the present study predicted that Karyopherin alpha-3 (KPNA3) is a potential target for miR-101. KPNA3, a subunit of the nuclear pore complex, has been documented to act importantly in the growth and metastasis of CRC cells.¹⁷⁻¹⁹ Thus, we assumed that SIRT1 may affect CRC progression and chemoresistance via regulation of the p53/miR-101/KPNA3 axis. Hence, we applied bioinformatics analysis, collected clinical samples and conducted an array of cellular and animal assays to justify the hypothesis.

Results

SIRT1 was upregulated in CRC tissues

Initial results of RT-qPCR and immunoblotting identified increased SIRT1 levels in CRC tissues (Figure 1a, b). Next, immunohistochemistry results depicted high SIRT1-positive expression in CRC tissues (Figure 1c). Furthermore, RT-qPCR displayed that SIRT1 mRNA level was elevated in CRC tissues of CRC patients at stage III than that in CRC tissues at stage I and II ($p = .001$)

CONTACT Xia Li  xiali_lx@126.com  Department of Anorectal Surgery, The First People's Hospital of Wenling, No. 333, Chuanan South Road, Chengxi Street, Wenling, Zhejiang Province 317500, China

 Supplemental data for this article can be accessed online at <https://doi.org/10.1080/15384047.2023.2235770>

© 2023 The Author(s). Published with license by Taylor & Francis Group, LLC.

This is an Open Access article distributed under the terms of the Creative Commons Attribution-NonCommercial License (<http://creativecommons.org/licenses/by-nc/4.0/>), which permits unrestricted non-commercial use, distribution, and reproduction in any medium, provided the original work is properly cited. The terms on which this article has been published allow the posting of the Accepted Manuscript in a repository by the author(s) or with their consent.

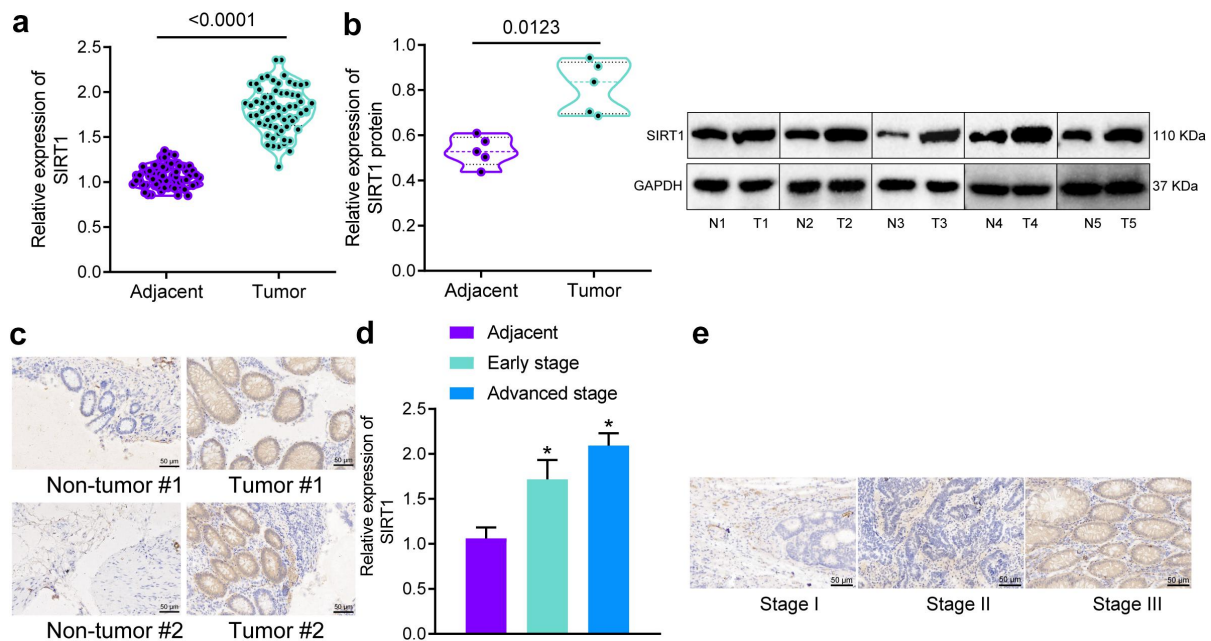


Figure 1. SIRT1 is highly expressed in CRC tissues. (a) SIRT1 mRNA level in CRC tissues and adjacent normal tissues determined using RT-qPCR, $n = 64$; (b) SIRT1 protein level in CRC tissues and adjacent normal tissues determined using Western blot analysis, $n = 5$; (c) SIRT1-positive expression in CRC tissues and adjacent normal tissues measured using immunohistochemistry ($\times 200$); (d) SIRT1 mRNA level in adjacent normal tissues and CRC tissues measured using RT-qPCR; (e) SIRT1-positive expression in adjacent normal tissues and CRC tissues measured using immunohistochemistry ($\times 200$). Values expressed as mean \pm standard deviation were analyzed by paired t test between CRC tissues and adjacent normal tissues and by ANOVA with Tukey's test among three or more groups. * $p < .05$ vs. adjacent normal tissues.

(Figure 1d). Immunohistochemistry demonstrated higher SIRT1-positive expression in CRC tissues at stage III than that in CRC tissues at stage I and II (Figure 1e). Taken together, SIRT1 was highly expressed in CRC tissues, and evidently upregulated in CRC patients at stage III.

Upregulation of SIRT1 facilitated cell malignant phenotypes in CRC cells

Subsequently, we determined SIRT1 expression in human CRC cell lines and normal colorectal epithelial cell line using RT-qPCR, which showed that SIRT1 expression was higher in LoVo and HCT116 cell lines, but lower in SW480 cell line than that in CCD-18Co cell line ($p = .039$) (Figure 2a). Thus, HCT116 cell line was treated with sh-SIRT1, and SW480 cell line was treated with oe-SIRT1.

We confirmed decreased SIRT1 expression in HCT116 cells treated with sh-SIRT1 and increased SIRT1 expression in SW480 cells treated with oe-SIRT1 (Figure 2b). Transwell assay proved inhibited cell migration and invasion in HCT116 cells after depletion of SIRT1, while the results were opposite in SW480 cells after restoration of SIRT1 (Figure 2c, d). Furthermore, Western blot analysis presented elevated E-cadherin and occluding levels but reduced vimentin, N-cadherin, and fibronectin levels in HCT116 cells after silencing of SIRT1 (Figure 2e). These findings implied that SIRT1 was abundantly expressed in CRC cells and elevated SIRT1 facilitated the migration, invasion, and epithelial-mesenchymal transformation (EMT) of CRC cells.

SIRT1-mediated deacetylation of p53 promoted cell malignant phenotypes in CRC cells

Subsequently, we further pinpointed the mechanism of SIRT1 regulating p53 in CRC. Western blot analysis results demonstrated that protein levels of p53 and acetylation of p53 (ac-p53) reduced in HCT116 cells (Figure 3a). IP assay displayed that depletion of SIRT1 inhibited the binding between SIRT1 and p53 (Figure 3b). The effect of SIRT1 on p53 expression was further examined, which revealed that the expression of ac-p53 and p53 increased after silencing of SIRT1 (Figure 3c).

Next, HCT116 cells were treated with $1 \mu\text{mol/L}$ Tenovin-6 (deacetylase inhibitor) to detect deacetylase cleavage activity of SIRT1, and the results presented that with the prolongation of Tenovin-6 treatment, deacetylase cleavage activity of SIRT1 was suppressed (Figure 3d). Moreover, SIRT1 expression diminished and expression of p53 and ac-p53 increased with the prolongation of Tenovin-6 treatment time (Figure 3e). Transwell assay presented that at 24 h after treatment with Tenovin-6, cell migration and invasion were repressed (Figure 3f). In addition, Western blot analysis results presented elevated E-cadherin and occluding levels but reduced vimentin, N-cadherin, and fibronectin levels in HCT116 cells treated with Tenovin-6 (Figure 3g). Furthermore, silencing of SIRT1 upregulated protein levels of E-cadherin and occluding while downregulating those of vimentin, N-cadherin and fibronectin (Figure 3h). Thus, SIRT1 reduced expression of p53 via mediation of deacetylation and thus promoted cell malignant features of CRC cells.

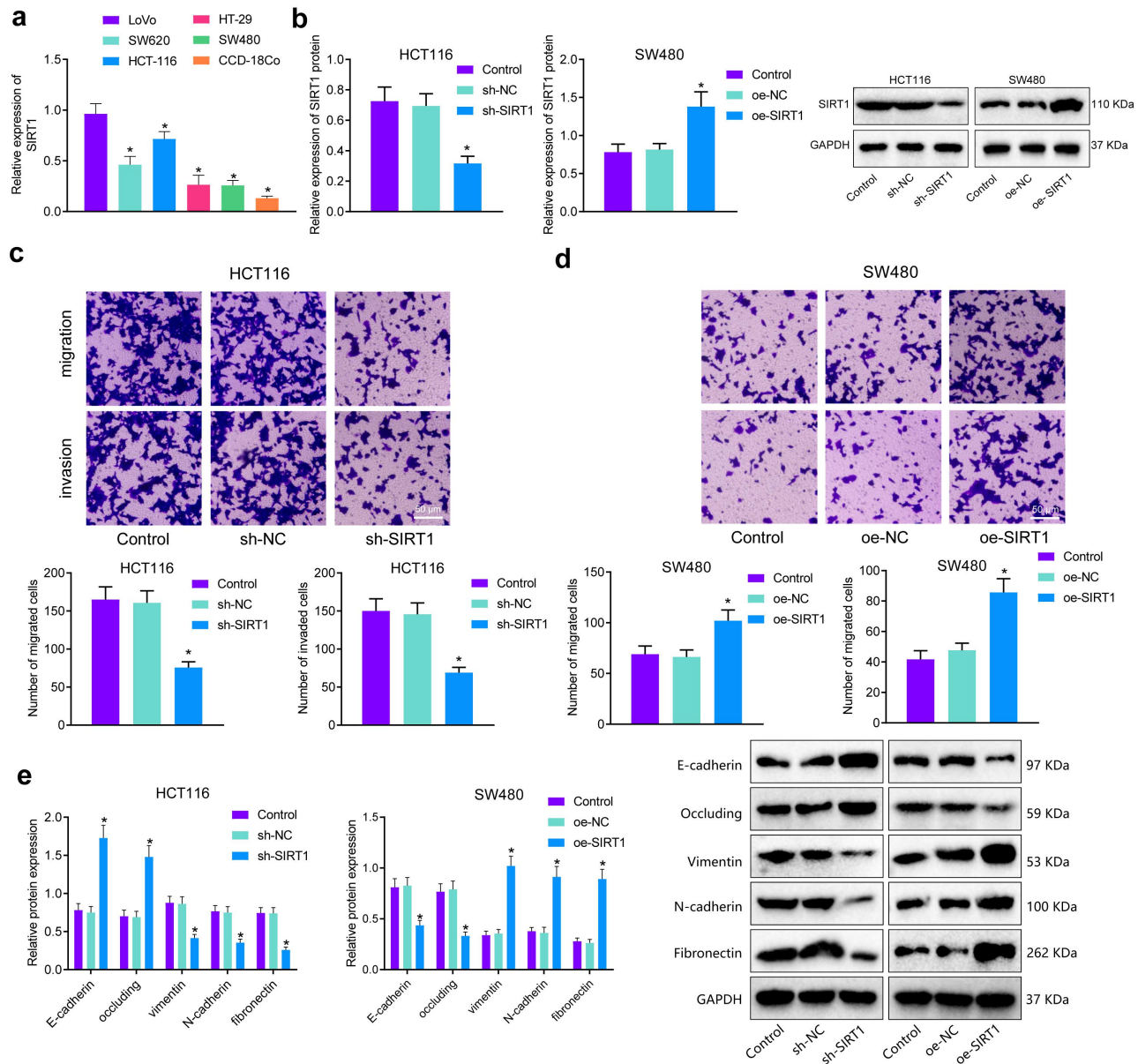


Figure 2. Overexpression of SIRT1 enhances cell migration, invasion, and EMT in CRC cells. (a) SIRT1 expression in five CRC cell lines LoVo, SW620, SW480, HCT-116, and HT-29 and normal colorectal epithelial cell line CCD-18Co determined using RT-qPCR; (b) SIRT1 expression in HCT116 cells treated with sh-SIRT1 and SW480 cells treated with oe-SIRT1 determined using RT-qPCR and Western blot analysis; (c) Migration and invasion of HCT116 cells treated with sh-SIRT1 detected using Transwell assay; (d) Migration and invasion of SW480 cells treated with oe-SIRT1 detected using Transwell assay; (e) Protein levels of EMT-related genes (E-cadherin, occluding, Vimentin, N-cadherin, and fibronectin) in HCT116 cells treated with sh-SIRT1 and SW480 cells treated with oe-SIRT1 determined using Western blot analysis. Values are expressed as mean \pm standard deviation and analyzed by ANOVA followed by Tukey's test among three or more groups. * $p < .05$ vs. CCD-18Co cell line, HCT116 cells treated with sh-NC or SW480 cells treated with oe-NC. The cell experiment was run in triplicate independently.

SIRT1 induced CRC cell malignant phenotypes by disturbing the p53/miR-101 axis

Next, the mechanism of SIRT1 in CRC was further explored. RT-qPCR data showed that miR-101 expression reduced in HCT116 cells relative to CCD-18Co cells (Figure 4a). HCT116 cells were treated with sh-p53 or oe-p53, and the results of RT-qPCR displayed that sh-p53 reduced the expression of p53 and miR-101, while oe-p53 exerted opposite effects (Figure 4b). To further verify whether SIRT1 could participate in the regulation of CRC progression by affecting miR-101 expression through p53, RT-qPCR was

conducted to measure miR-101 expression in HCT116 cells after knockdown of SIRT1. The results depicted that silencing of SIRT1 elevated miR-101 expression, while further silencing of p53 reduced miR-101 expression (Figure 4c), suggesting that SIRT1 regulated p53 to affect miR-101 expression in CRC cells.

Furthermore, HCT116 cells were treated with miR-101 mimic (Figure 4d). miR-101 mimic was found to repress HCT116 cell migration and invasion (Figure 4e). Western blot analysis presented elevated E-cadherin and occluding but reduced those of vimentin, N-cadherin, and fibronectin

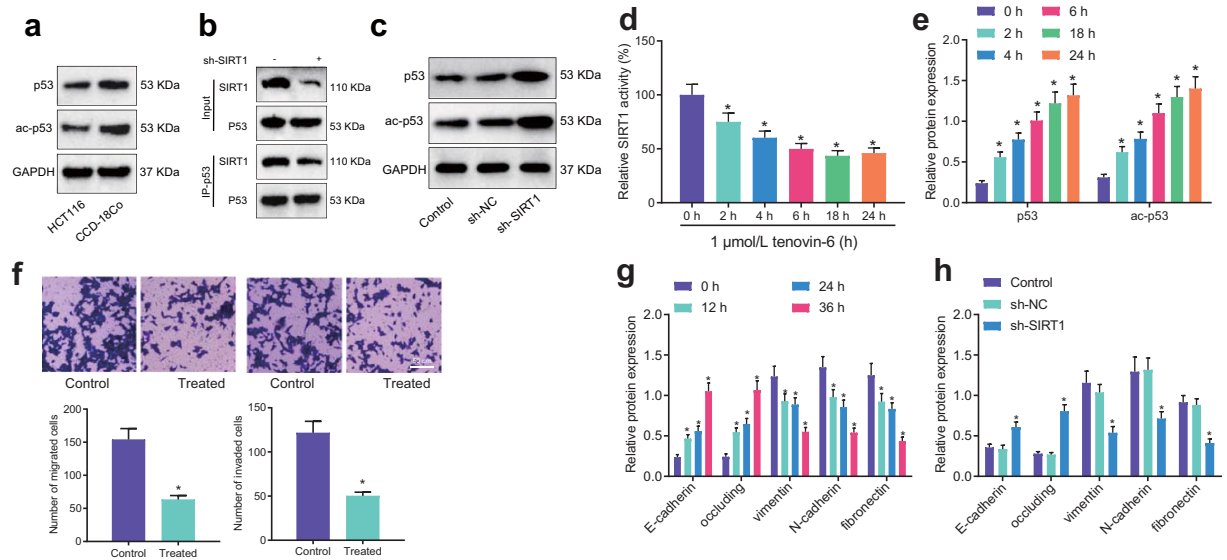


Figure 3. SIRT1 downregulates the expression of p53 via deacetylation and facilitates cell migration, invasion and EMT in CRC cells. (a) Protein levels of p53 and ac-p53 in five CRC cell line HCT-116 and normal colorectal epithelial cell line CCD-18Co measured using Western blot analysis; (b) the binding between SIRT1 and p53 detected using IP assay; (c) the effect of SIRT1 on p53 expression detected using Western blot analysis; (d) Deacetylase cleavage activity of SIRT1 in HCT116 cells treated with 1 $\mu\text{mol/L}$ Tenovin-6 at 0, 2, 4, 6, 18, 24 h; (e) Expression of p53 and ac-p53 in HCT116 cells treated with 1 $\mu\text{mol/L}$ Tenovin-6 at 0, 2, 4, 6, 18, 24 h detected using Western blot analysis; (f) Cell migration and invasion in HCT116 cells treated with 1 $\mu\text{mol/L}$ Tenovin-6 at 0, 2, 4, 6, 18, 24 h detected using Transwell assay; (g) Protein levels of EMT-related genes (E-cadherin, occluding, Vimentin, N-cadherin, and fibronectin) in HCT116 cells treated with 1 $\mu\text{mol/L}$ Tenovin-6 at 0, 2, 4, 6, 18, 24 h detected using Western blot analysis. (h) Protein levels of EMT-related genes (E-cadherin, occluding, Vimentin, N-cadherin, and fibronectin) in HCT116 cells treated with sh-SIRT1 detected using Western blot analysis. Values are expressed as mean \pm standard deviation and analyzed by unpaired *t* test between two groups and by ANOVA followed by Tukey's test among three or more groups. **p* < .05 vs. HCT116 cells or HCT116 cells treated with 1 $\mu\text{mol/L}$ Tenovin-6 at 0 h. The cell experiment was run in triplicate independently.

in HCT116 cells in the presence of miR-101 mimic (Figure 4f). Therefore, SIRT1 was demonstrated to downregulate the p53/miR-101 axis to promote CRC cell migration, invasion, and EMT.

KPNA3 was a putative target of miR-101 in CRC cells

Differential analysis of the GSE68204 dataset revealed 66 DEGs (Figure 5a). The results of GO enrichment analysis using Panther pinpointed that the DEGs were mainly concentrated in six items, and mostly enriched in the GO: 0005488, which included 15 DEGs (Figure 5b). After comparison of logFC and *p* value among 15 DEGs, NEUROG1, REG1B, CMIP, and KPNA3 were identified, of which correlation between KPNA3 and drug resistance of tumor cells has not been reported. Thus, KPNA3 was a novel target and selected for the follow-up study.

Through differential analysis of the GSE68204 dataset, KPNA3 was highly expressed in drug-resistant samples of CRC (Figure 5c). GEPIA database also verified increased KPNA3 expression in CRC samples (Figure 5d). RT-qPCR data showed increased KPNA3 expression in CRC tissues (*p* = .001) (Figure 5e). Immunohistochemistry also proved that KPNA3 positive expression was increased in CRC tissues (Figure 5f). Following intersection analysis of the upstream regulatory miRNAs of DEGs predicted using starBase, miRDB, miRanda, and mirDIP databases, eight miRNAs (hsa-miR-101-3p, hsa-miR-24-3p, hsa-miR-19a-3p, hsa-miR-19b-3p, hsa-miR-93-5p, hsa-miR-15a-5p, hsa-miR-16-5p, and hsa-miR-27a-3p) were identified (Figure 5g). The starBase database displayed the binding sites between miR-101 and KPNA3

(Figure 5h). In addition, the luciferase activity of KPNA3 3'UTR-WT instead of KPNA3 3'UTR-Mut was diminished in the presence of miR-101 mimic (Figure 5i), indicating that miR-101 targeted KPNA3. Furthermore, KPNA3 expression was repressed in the presence of miR-101 mimic (*p* = .001) (Figure 5j). Therefore, miR-101 can target KPNA3 and negatively regulate its expression in CRC cells

Overexpression of KPNA3 increased the chemoresistance of CRC cells to 5-FU

HCT116 cells were treated with sh-KPNA3 or oe-KPNA3. As detected by RT-qPCR and immunoblotting, sh-KPNA3 reduced KPNA3 expression, while oe-KPNA3 displayed the opposite results (*p* = .001) (Figure 5k). MTT assay presented that 5-FU led to inhibited cell viability in HCT116 cells treated with sh-KPNA3, while the results were opposite in HCT116 cells treated with oe-KPNA3 (*p* = .001) (Figure 5i). In addition, overexpression of KPNA3 increased IC50 value of HCT116 cells, and knockdown of KPNA3 decreased IC50 value of HCT116 cells (*p* = .001) (Figure 5m). These findings implied that KPNA3 could promote the resistance of CRC cells to 5-FU but knockdown of KPNA3 reversed this effect.

SIRT1 induced CRC cell chemoresistance to 5-FU and promoted cell migration, invasion, and EMT via the p53/miR-101/KPNA3 axis

Then, we aimed to further investigate whether SIRT1 regulating KPNA3 expression affected the resistance of CRC cells to 5-FU. SIRT1 knockdown in HCT116 cells inhibited KPNA3

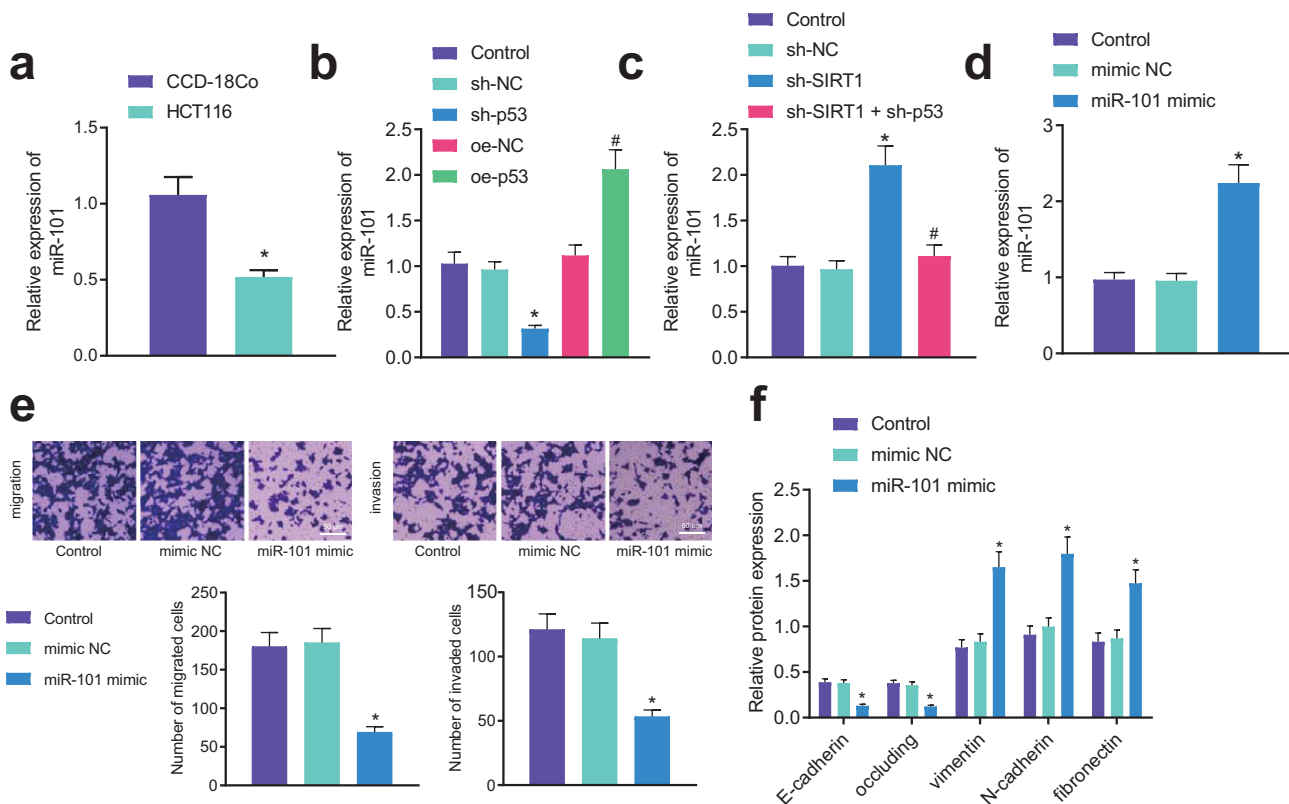


Figure 4. SIRT1 promotes CRC cell migration, invasion, and EMT *via* suppression of the p53/miR-101 axis. (a) miR-101 expression in HCT116 and CCD-18Co cells determined using RT-qPCR; (b) Expression of p53 and miR-101 in HCT116 cells treated with sh-p53 or oe-p53 determined using RT-qPCR; (c) miR-101 expression in HCT116 cells treated with miR-101 mimic determined using RT-qPCR; (e) Cell migration and invasion in HCT116 cells treated with miR-101 mimic detected using Transwell assay; (f) Protein levels of EMT-related genes (E-cadherin, occluding, Vimentin, N-cadherin, and fibronectin) in HCT116 cells treated with miR-101 mimic measured using Western blot analysis. Values are expressed as mean \pm standard deviation and analyzed by unpaired *t* test between two groups and by ANOVA followed by Tukey's test among three or more groups. **p* < .05 vs. CCD-18Co cells, HCT116 cells treated with sh-NC or HCT116 cells treated with mimic NC. The cell experiment was run in triplicate independently.

expression (Figure 6a). MTT assay revealed that silencing of SIRT1 reduced HCT116 cell viability and IC₅₀ value (Figure 6b, c). Further overexpression of KPNA3 augmented HCT116 cell viability and IC₅₀ value (Figure 6b, c). Moreover, overexpression of KPNA3 facilitated HCT116 cell migration and invasion, but additional silencing of SIRT1 failed to augment the cell migration and invasion evidently (Figure 6d).

Western blot analysis revealed that overexpressed KPNA3 elevated E-cadherin and occluding levels but suppressed those of vimentin, N-cadherin, and fibronectin; however, additional silencing of SIRT1 led to no considerable changes in the expression of these proteins (Figure 6e). These findings confirmed that SIRT1 modulated the p53/miR-101/KPNA3 axis to facilitate the migration, invasion, EMT and chemoresistance of CRC cells.

SIRT1 accelerated the growth, metastasis and chemoresistance to 5-FU of CRC cells via the p53/miR-101/KPNA3 axis *in vivo*

At last, nude mice models of subcutaneous transplanted tumors were established with HCT116 cells with depleted SIRT1 and SW480 cells with elevated SIRT1 to explore effects of SIRT1 on the growth, metastasis and chemoresistance to 5-FU of CRC cells via the p53/miR-101/KPNA3 axis *in vivo*. Nude mice injected with HCT116 cells with depleted SIRT1 exhibited

reduced number of metastatic foci in the lung and liver (Figure 7a), while overexpression of SIRT1 increased the number of metastatic foci in the lung and liver (Figure 7b). Immunohistochemistry revealed diminished expression of SIRT1 and KPNA3 and increased p53 expression in the tumor tissues of nude mice injected with HCT116 cells treated with sh-SIRT1, while the results were opposite in the presence of SIRT1 overexpression (Figure 7c). RT-qPCR showed elevated miR-101 expression in the tumor tissues of nude mice injected with HCT116 cells with depleted SIRT1, while the results were opposite following SIRT1 overexpression (Figure 7d).

After intraperitoneal injection of 5-FU into nude mice treated with oe-SIRT1, tumor volume and weight obviously elevated (Figure 7e), suggesting that elevated SIRT1 promoted the chemoresistance of CRC cells *in vivo*. Besides, Western blot analysis presented elevated E-cadherin and occluding levels but reduced vimentin, N-cadherin, and fibronectin levels in the tumor tissues of nude mice injected with HCT116 cells overexpressing SIRT1 (Figure 7f). These results confirmed that SIRT1 promoted the growth, metastasis and chemoresistance to 5-FU of CRC cells via the p53/miR-101/KPNA3 axis *in vivo*.

Discussion

Over the past decades, 5-Fu is widely used in the treatment for CRC, while the resistance to 5-Fu remains a major problem.²⁰

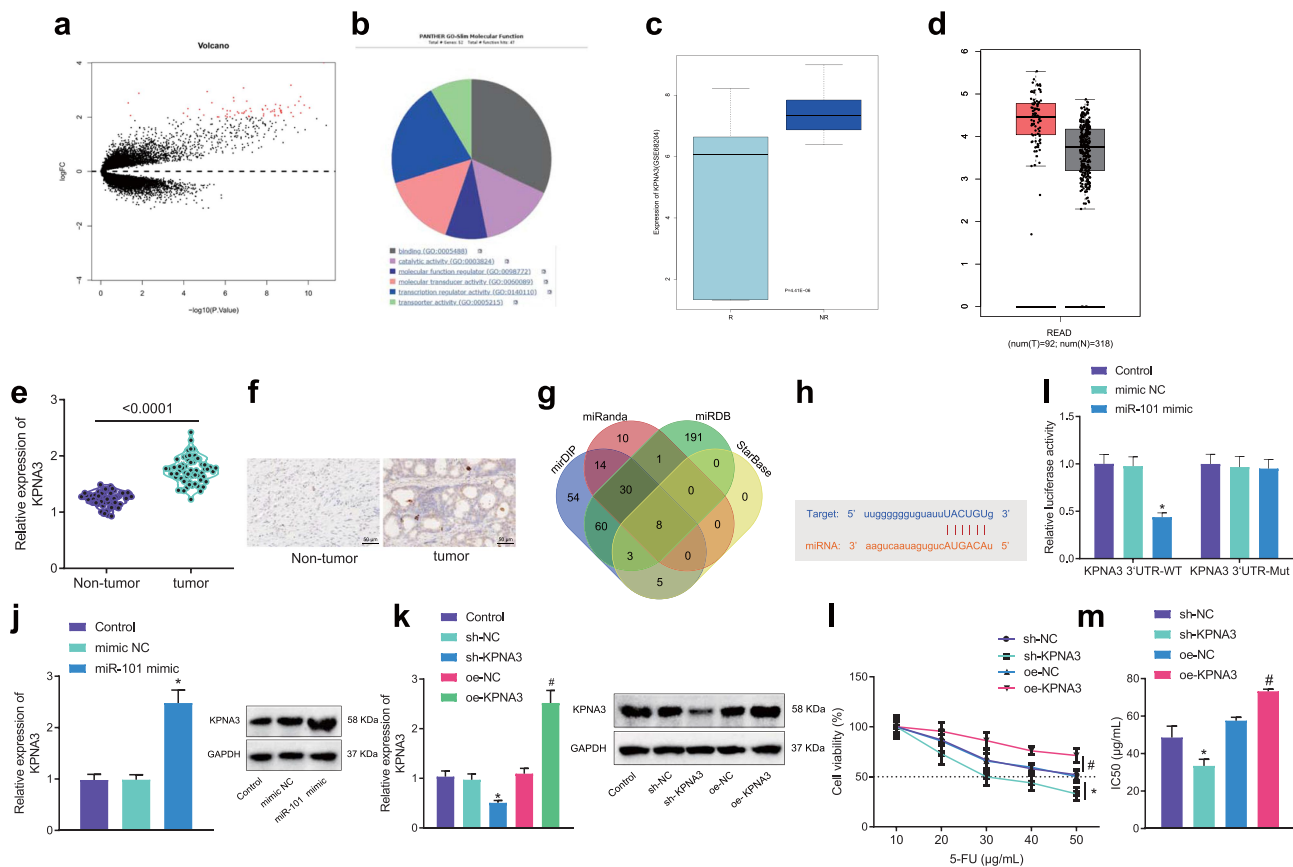


Figure 5. MiR-101 promoted the chemoresistance of CRC cells to 5-FU by targeting KPNA3. (a) A volcano map of the DEGs from the GSE68204 dataset. The abscissa indicates the $\log_{10} p$ value and the ordinate indicates $\log_{2}FC$. Each dot represents a gene, the red dot represents upregulated genes, and the green dot represents downregulated genes in drug-resistant samples. (b) GO functional enrichment of DEGs; (c) A box plot of KPNA3 expression in CRC samples in the GSE68204 dataset; (d) a box plot of KPNA3 expression in CRC samples in TCGA database; (e) KPNA3 expression in CRC tissues and adjacent normal tissues determined using RT-qPCR, $n = 64$; (f) KPNA3 expression in CRC tissues and adjacent normal tissues determined using immunohistochemistry; (g) Venn diagram of miRNas that regulated DEGs predicted by the starBase, miRDB, miRanda and miRIP databases; (h) Binding sites between miR-101 and KPNA3 predicted using starBase; (i) Binding of miR-101 to KPNA3 detected using dual luciferase reporter assay; (j) KPNA3 expression in HCT116 cells treated with miR-101 mimic determined using RT-qPCR and Western blot analysis; (k) KPNA3 expression in HCT116 cells treated with sh-KPNA3 or oe-KPNA3 determined using RT-qPCR and Western blot analysis; (l) HCT116 cell viability after treatment with 5-FU at different concentrations (10, 20, 30, 40 and 50 $\mu\text{g/mL}$) detected by MTT assay; (m) IC₅₀ value in HCT116 cells treated with sh-KPNA3 or oe-KPNA3. Values are expressed as mean \pm standard deviation and analyzed by paired t test between CRC tissues and adjacent normal tissues, by unpaired t test between two groups, and by ANOVA followed by Tukey's test among three or more groups. * $p < .05$ vs. adjacent normal tissues, or HCT116 cells treated with sh-NC or mimic NC; # $p < .05$ vs. HCT116 cells treated with oe-NC. The cell experiment was run in triplicate independently.

Our study probed into the effect of SIRT1 on CRC cells to 5-FU-based chemotherapy based on in vitro and in vivo experiments. The obtained results elucidated that SIRT1 could promote CRC progression and chemoresistance to 5-Fu by regulating the p53/miR-101/KPNA3 axis.

Initial data of our work depicted that SIRT1 was highly expressed in CRC tissues and cell lines. In addition, the upregulation of SIRT1 could facilitate the migration, invasion, EMT and chemoresistance of CRC cells. Consistently, published literature has indicated that inhibiting the expression of SIRT1 contributes to reduced CRC cell viability and autophagy yet promoted cell apoptosis.²¹ SIRT1 expression is elevated in CRC tissues and the autophagy mediated by SIRT1 can promote the chemoresistance of CRC to 5-Fu.¹¹ Another study has also identified the upregulated SIRT1 expression in CRC, and that this upregulation facilitates CRC cell migration and invasion.⁸ Thus, these findings support that SIRT1 inhibition may be a promising target for CRC treatment.

In addition, our data clarified that miR-101 expression decreased in CRC. The aberrant expression of miRNAs is involved in CRC by modulating their target genes.¹⁵

Reduced miR-101 has been validated in the CRC previously, which contributes to tumor invasiveness.²² Moreover, our work unveiled that miR-101 targeted KPNA3, and miR-101 inhibited cell migratory and invasive capacities, EMT, and chemoresistance to 5-FU by inhibiting KPNA3 in CRC cells. Jiang et al. have also proved that miR-101 expression is diminished in CRC, and restored miR-101 limits the EMT and metastasis of CRC cells.¹⁶ Meanwhile, miR-101 acts to repress CRC as elevated miR-101 hampers the aggressive behaviors of CRC in vivo.²³ miR-101-3p overexpression is capable of decreasing the resistance of CRC to irradiation,²⁴ while the inhibiting role of miR-101 in CRC chemoresistance has not been explored. Furthermore, silencing of KPNA3 results in inhibition of cell malignant phenotypes in CRC.¹⁹ Emerging evidence demonstrates that miRNAs can interact with the 3'UTR of specific target mRNAs and lead to the repression of their expression.^{25,26} This study clarifies the first evidence for the post-transcriptional modulation of KPNA3 by miR-101 in CRC cells and the miR-101/KPNA3 axis might have significance in the regulation of CRC progression.

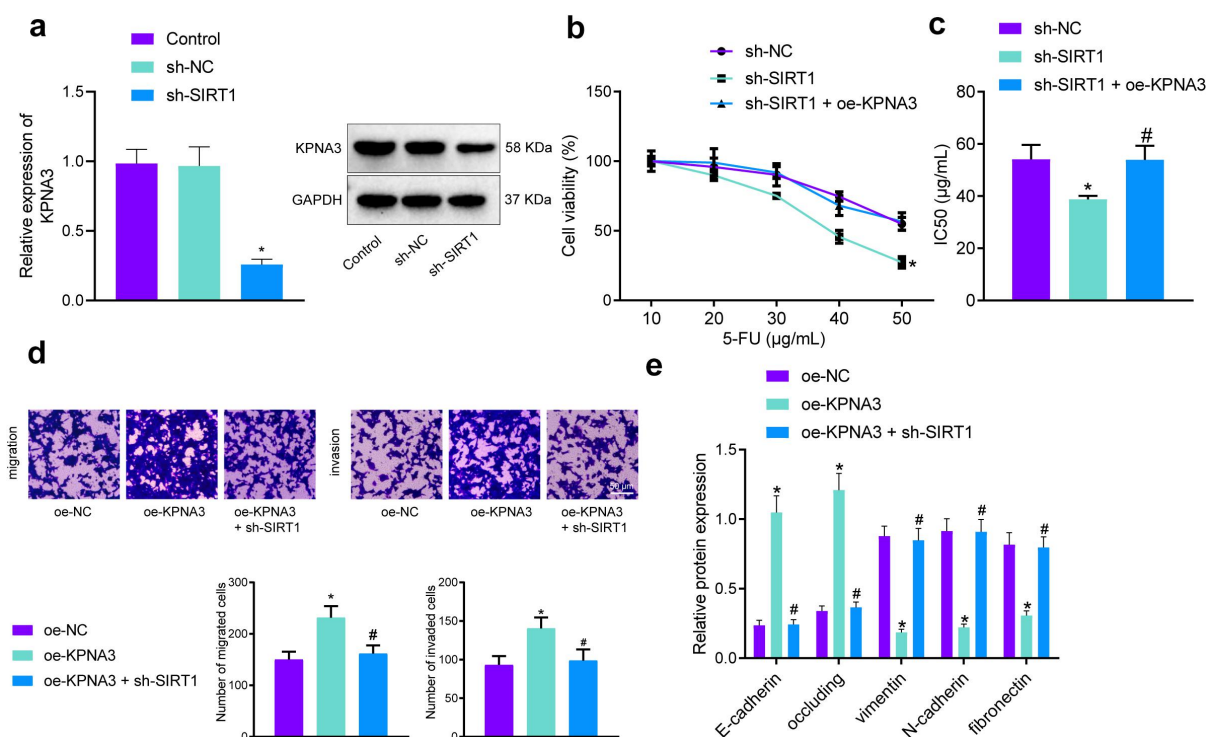


Figure 6. SIRT1 induces the migration, invasion, EMT and chemoresistance of CRC cells via the p53/miR-101-KPNA3 axis. (a) KPNA3 expression in HCT116 cells treated with sh-SIRT1 measured using RT-qPCR and Western blot analysis; (b) HCT116 cell viability following treatment with sh-SIRT1 or combined with oe-KPNA3 detected using MTT assay; (c) IC₅₀ value in HCT116 cells treated with sh-SIRT1 or combined with oe-KPNA3 measured using MTT assay; (d) HCT116 cell migration and invasion following treatment with oe-KPNA3 or combined with sh-SIRT1 detected using Transwell assay; (e) Protein levels of EMT-related genes (E-cadherin, occluding, Vimentin, N-cadherin, and fibronectin) in HCT116 cells treated with oe-KPNA3 or combined with sh-SIRT1 measured using Western blot analysis. Values are expressed as mean ± standard deviation and analyzed by ANOVA followed by Tukey's test among three or more groups and by repeated measures ANOVA followed by Bonferroni's test at different time points. * $p < .05$ vs. HCT116 cells treated with sh-NC or oe-NC; # $p < .05$ vs. HCT116 cells treated with sh-SIRT1 or oe-KPNA3. The cell experiment was run in triplicate independently.

What's more, SIRT1 facilitated chemoresistance, migration, invasion, and EMT of CRC cells via the p53/miR-101/KPNA3 axis in our study. EMT, as one of the crucial molecular steps in distant metastasis, is the main cause of CRC-related death, and shares correlation with a poor prognosis in CRC.²⁷ EMT is manifested with the reduction of E-cadherin and occluding and elevation of vimentin and fibronectin, and depletion of SIRT1 could reduce vimentin level and elevates E-cadherin level,⁸ suggesting that SIRT1 contributes to increase of CRC cell metastasis regulated by EMT. A recent study has also implied that CRC resistance to the 5-FU remains a major problem in CRC treatment, and SIRT1 acts as an oncogene in mechanisms of CRC resistance to 5-FU.¹¹ It also known that anti-cancer efficacy of 5-FU in CRC cellular processes can be produced through p53.²⁸ SIRT1 can modulate p53 deacetylation.²⁹ SIRT1 mediates deacetylation of p53 so as to inhibit the activity of p53 and tumorigenesis of CRC, which suggests that silencing of SIRT1 leads to activation of p53 and impedes CRC progression.¹³ The activation of p53 and miR-101 is also proved as a potential therapy in cancer.¹⁴ Herein, it is reasonable that SIRT1-mediated deacetylation of p53 possessed with great therapeutic potential in CRC progression and chemoresistance to 5-Fu via miR-101/KPNA3.

In conclusion, this study is the first to reveal that SIRT1 plays an oncogenic role in CRC cell growth and metastasis as well as chemoresistance via deacetylation of p53, inhibition of

miR-101 expression and upregulation of KPNA3 expression (Figure 8). Thus, targeting the SIRT1/p53/miR-101/KPNA3 axis may function as an appealing direction for creating therapeutic modalities for CRC. However, more experiments are necessitated to further explore the intrinsic mechanisms.

Materials and methods

Ethics statement

Our work was performed with the approval of the Academic Ethics Committee of The First People's Hospital of Wenling and performed on the basis of the Declaration of Helsinki. All participants signed informed consent documentation. Animal experimentations were ratified by the Academic Ethics Committee of The First People's Hospital of Wenling and implemented on the basis of the Animal Welfare Legislation in China and ARRIVE Guidelines.

In silico analysis

CRC-related mRNA expression dataset GSE68204 and miRNA expression dataset GSE30454 were downloaded from GEO database. GSE68204 contains 27 chemotherapy-sensitive CRC patients and 32 chemotherapy-resistant CRC patients. GSE30454 contains 20 normal colorectal tissue samples and 54

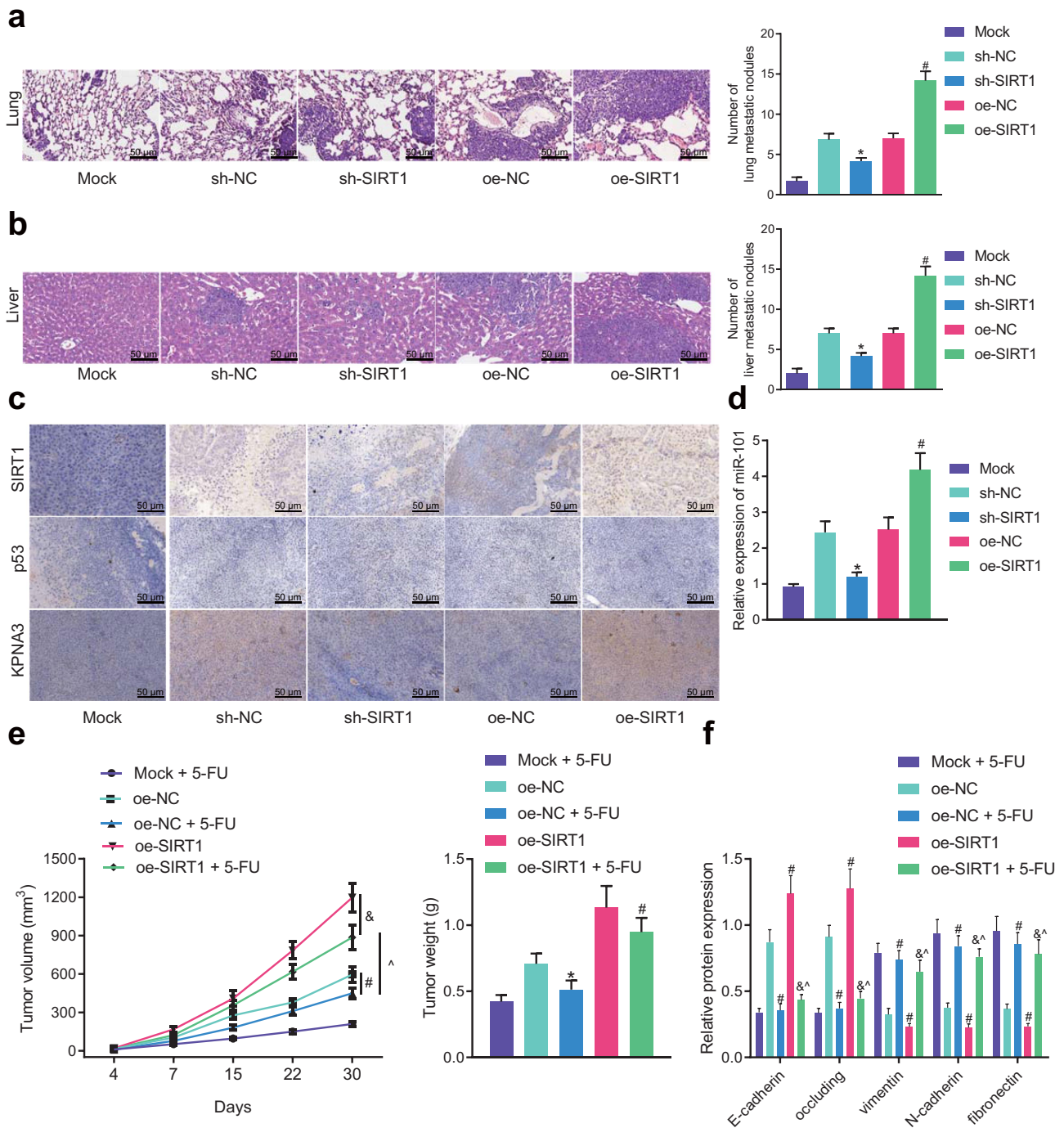


Figure 7. SIRT1 accelerates the growth, metastasis and chemoresistance to 5-FU of CRC cells via the p53/miR-101-KPNA3 axis *in vivo*. Nude mice were injected with HCT116 cells with depleted SIRT1 (with sh-NC plasmids as control) or elevated SIRT1 (with oe-NC plasmids as control). (a) Metastatic lung tumors in nude mice detected using HE staining (×200); (b) Metastatic liver tumors in nude mice detected using HE staining (×200); (c) Expression of SIRT1, p53, and KPNA3 in the tumor tissues of mice determined using immunohistochemistry (×200); (d) miR-101 expression in the tumor tissues of mice determined using RT-qPCR; (e) Tumor volume and weight of oe-SIRT1-treated mice intraperitoneally injected with 5-FU; (f) Protein levels of EMT-related genes (E-cadherin, occludin, Vimentin, N-cadherin, and fibronectin) in tumor tissues of oe-SIRT1-treated mice intraperitoneally injected with 5-FU measured using Western blot analysis. Values are expressed as mean ± standard deviation and analyzed by ANOVA followed by Tukey's test among three or more groups and by repeated measures ANOVA followed by Bonferroni's test at different time points. * $p < .05$ vs. mice treated with sh-NC; # $p < .05$ vs. mice treated with oe-NC.

CRC tissue samples. R “limma” package was processed for differential analysis to identify the differentially expressed mRNAs related to the development and chemoresistance of CRC with $|\log_2FC| > 2$ and p value $< .05$ as the threshold which were then subjected to GO enrichment analysis.

Next, the upstream regulatory miRNAs of the differentially expressed genes were predicted through the starBase, miRDB, miRanda and mirDIP databases, which were then intersected. Finally, the KEGG database was used to retrieve the upstream regulatory factors of the predicted upstream miRNAs,

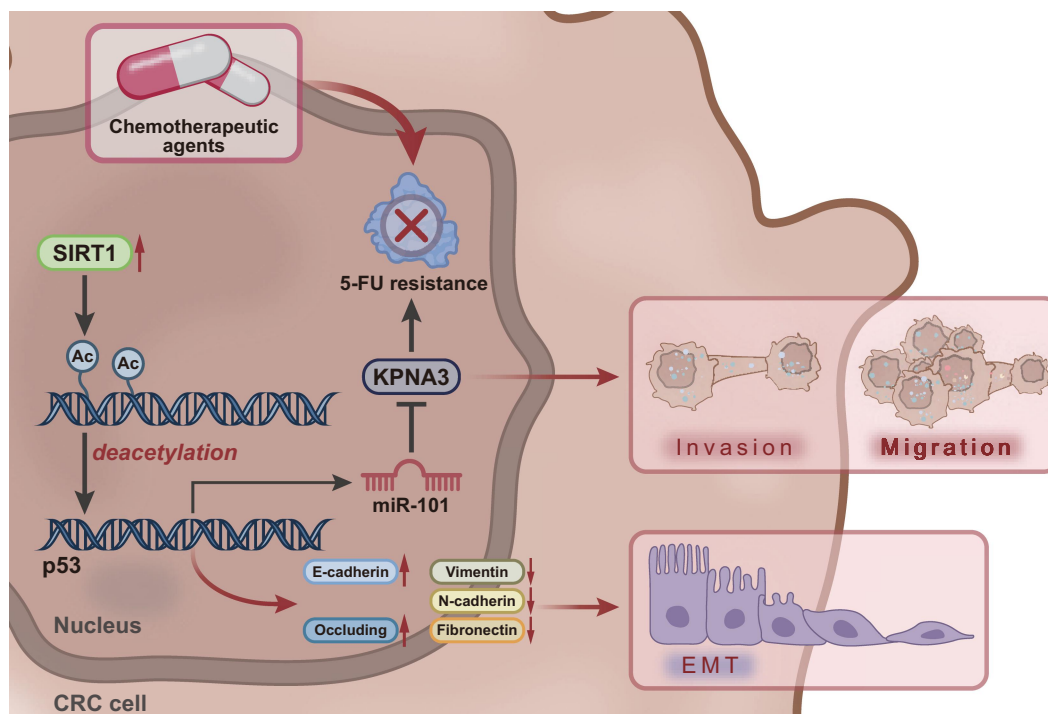


Figure 8. Systematic diagram depicting that the molecular mechanism of SIRT1 influencing CRC development and chemoresistance to 5-FU. SIRT1 promotes deacetylation of p53 and inhibits the expression of p53, thus reducing the expression of miR-101 while upregulating that of the miR-101 target gene KPNA3. By this mechanism, the growth, metastasis and chemoresistance to 5-FU of CRC cells are promoted.

followed by construction of a transcription factor-miRNA-mRNA co-expression regulatory network.

Tissue collection

Primary CRC and adjacent normal tissue samples were harvested from 64 patients with CRC (39 males and 25 females) who received surgery at The First People's Hospital of Wenling. There were 30 patients under 60 y old and 34 patients over 60 y old. Moreover, there were 12 patients at stage I, 37 patients at stage II, and 15 patients at stage III. The included patients were confirmed as CRC by postoperative pathology. All specimens were evaluated according to World Health Organization guidelines and pathological staging criteria of the Union for International Cancer Control.³⁰ All specimens were frozen in liquid nitrogen and preserved at -80°C .

Cell culture and grouping

Human CRC cell lines, LoVo, SW620, SW480, HCT-116, and HT-29, normal colorectal epithelial cell line, CCD-18Co and HEK293T cells were procured from ATCC (Manassas, VA). These cells were incubated in DMEM (25 mM D-glucose, 1 mM sodium pyruvate and 4 mM L-glutamine (Gibco, Carlsbad, CA) replenished with 10% FBS (Biological Industries USA, Inc., CT) and 1% penicillin-streptomycin (Gibco).

Lentiviral packaging LV5-GFP and pSIH1-H1-copGFP were used to transmit overexpressing and shRNA sequences, respectively. sh-SIRT1, sh-p53, sh-KPNA3, negative control (NC) shRNA (sh-NC), miR-101 mimic, and mimic NC were from GenePharma Co. Ltd. (Shanghai, China). The packaging lentivirus and target vectors were co-transfected into

HEK293T cells employing Lipofectamine 2000. Following incubation for 48 h, supernatants were collected to detect viral titer, followed by infection of CRC cells.

Immunohistochemistry

Paraffin-embedded human CRC tissues were cut into serial 4- μm sections, which were antigen-retrieved and blocked with normal goat serum. Next, the sections were stained using HistostainTMS-9000 Immunohistochemical Staining Kit (Zymed Laboratories, San Francisco, CA). The sections were immunostained with primary rabbit antibodies (Abcam Inc. Cambridge, MA) to SIRT1 (ab110304, 1:100), p53 (ab131442, 1:100), and KPNA3 (ab6038, 1:100) at 4°C overnight. The sections were re-probed with rat anti-rabbit antibody (ab6728, 1:1000, Abcam) at 37°C for 30 min. The samples were developed by DAB for 5–10 min, and photographed under an inverted microscope (NIB900, Nexcopy Inc., CA). The cells showing brown and yellow cytoplasm were described as positive.

RNA isolation and quantitation

Employing a TRIzol reagent (Invitrogen, Carlsbad, California), total RNA was extracted and 400 ng of which was reversely transcribed into cDNA employing the PrimeScript RT Reagent Kit (Takara Bio Inc., Otsu, Shiga, Japan). With the help of the SYBR[®] Premix Ex Taq[™] II (Tli RNaseH Plus) kit (Takara), the Thermal Cycler Dice Real Time System Amplifier (Takara) was adopted for RT-qPCR. The primer sequences (Supplementary Table 1) were

synthesized by Guangzhou RiboBio Co., Ltd. (Guangzhou, China). GAPDH served as the internal reference and the expression of gene of interest was calculated with the $2^{-\Delta\Delta Ct}$ method.

Transwell assay

Transwell chamber (pore size of 8 mm; Corning Incorporated, Corning, NY) coated with or without Matrigel in 24-well plates was adopted for CRC cell migration and invasion measurement.³¹ Cells were subjected to observation and calculation under an inverted microscope in five high power fields.

Immunoblotting

Total protein extracts were separated and transferred onto membranes which were incubated with primary antibodies (Abcam) against SIRT1 (ab110304, 1:1000), p53 (ab131442, 1:1000), KPNA3 (ab6038, 1:1000), and GAPDH (ab37168, 1:1000, loading control) at 4°C overnight. Subsequently, the membrane was supplemented with HRP-labeled goat anti-mouse or goat anti-rabbit antibody (HS101, 1:1000, Beijing TransGen Biotech Co., Ltd., Beijing, China) for 1 h. Thereafter, ECL reagent was used for visualization of the immunocomplexes, and band intensities were assayed employing ImageJ.

SIRT1 catalytic activity measurement

A fluorometric activity assay kit (Sigma) was adopted for quantifying SIRT1 deacetylase activity. Samples were placed to a Costar 96-well dark plate, followed by detection of the deacetylation-dependent fluorescent signal employing a fluorescent reader (excitation wavelength of 360 nm, emission wavelength of 460 nm).

Dual luciferase reporter assay

The psiCHECK-2 vector (0.1 µg, Promega, Madison, WI) was adopted to build the firefly luciferase reporter vectors. The KPNA3 3'UTR-WT and KPNA3 3'UTR-Mut were co-transfected into the HEK293T cells in the presence of miR-101 mimic or NC mimic using X-tremegene HP (Roche Diagnostics GmbH, Mannheim, Germany). Following 48 h of transfection, the Dual-Luciferase Reporter Assay System (Promega) was run for luciferase activity measurement.

MTT assay

CRC cells were seeded into 96-well plates (10,000 cells/well; 100 µL) and incubated for 12 h. The cells were treated with 5-FU at different concentrations, and incubated with 20 µL of MTT (5 mg/mL in PBS, Sigma) for 4 h. Next, DMSO (200 µL) was supplemented to dissolve the crystals. The optical density (OD) value at 490 nm was assayed employing a microplate reader.

Immunoprecipitation (IP) assay

Cell lysate was subjected to treatment for protein collection for IP. Then, the harvested protein was incubated with flag

or p53 antibody (anti-IgG as NC) at 4°C overnight, and cultured with protein A/G beads for 4 h. Following three times of PBS washing, the beads were solubilized in SDS sample buffer, followed by immunoblotting with corresponding antibodies.

Construction of a xenograft model of CRC and a metastasis model

Totally 30 male BALB/c nude mice (6 weeks old; 13–17 g; Beijing Vital River Laboratory Animal Technology Co., Ltd., Beijing, China) were used for *in vivo* assays. The mice were assigned into five groups ($n = 6$ for each group): Mock + 5-FU (intraperitoneal injection with 50 mg/kg 5-FU, 50 mg every other day), oe-NC (subcutaneous inoculation of 1×10^7 CRC cells transduced with lentivirus harboring oe-NC into the dorsal side of mice), oe-NC + 5-FU (subcutaneous inoculation of 1×10^7 CRC cells transduced with lentivirus harboring oe-NC into the dorsal side of mice and intraperitoneal injection with 50 mg/kg 5-FU, 50 mg every other day), oe-SIRT1 (subcutaneous inoculation of 1×10^7 CRC cells transduced with lentivirus carrying oe-SIRT1 into the dorsal side of mice) and oe-SIRT1 + 5-FU (subcutaneous inoculation of 1×10^7 CRC cells transduced with lentivirus carrying oe-SIRT1 into the dorsal side of mice and intraperitoneal injection with 50 mg/kg 5-FU, 50 mg every other day). Tumor size was recorded every other day and measured using Vernier calipers, followed by tumor volume calculation. After 30 d of treatment, mice were euthanized by injecting triple doses of 3% sodium pentobarbital (P3761, Sigma), and tumors were removed and weighed.

In order to observe the lung and liver metastases in mice, HCT116 cells ($1 \times 10^7/0.2$ mL) overexpressing and silencing SIRT1 were injected into the lateral tail vein and subsplenic capsule of mice. After 10 weeks, mice were euthanized using the same method as the above. The liver and lung metastases were observed by HE staining, and the number of metastases on the lung and liver surfaces of each nude mouse was determined. The number of metastatic foci in the lung and liver was analyzed under a dissecting microscope.

Statistical analysis

Measurement data, analyzed by SPSS 21.0 software, were summarized as mean \pm standard deviation. Statistical significance was assayed employing paired *t*-test or unpaired *t*-test (two-group data with normal distribution and equal variance), one-way ANOVA with Tukey's test (multigroup data) or repeated measures ANOVA (time-based multigroup data) with Bonferroni's test. $p < .05$ was statistically significant.

Disclosure statement

The authors declare no conflict of interest.

Funding

The author(s) reported there is no funding associated with the work featured in this article.

Notes on contributors

Xiao-Wei Wang Graduated in 2012 with a master's degree from Zhejiang Medical University. Since 2012, he has been working at Wenling City First People's Hospital in the Colorectal Surgery Department. His research focus is on colorectal malignancies and common anorectal diseases.

Ying-Hao Jiang Graduated in 2015 with a master's degree from Zhejiang Medical University. From 2015 to the present, he has been working at Wenling City First People's Hospital in the Colorectal Surgery Department. He specializes in colorectal cancer and common anorectal diseases.

Wei Ye Graduated with an associate degree from Wenzhou Medical College in 1995 and with a bachelor's degree from Zhejiang Medical University in 2005. She has been working in the Colorectal Surgery Department at Wenling City First People's Hospital since 1995. Her research focuses on colorectal malignancies, challenging anorectal conditions, and common diseases.

Chun-Fa Shao Graduated with an associate degree from Wenzhou Medical College in 1997 and with a bachelor's degree from Zhejiang Medical University in 2003. From 1997 to 2000, he worked at Wenling City's Wenxi Central Health Clinic. Since 2000, he has been employed at Wenling City First People's Hospital in the Colorectal Surgery Department. He researches challenging anorectal conditions, malignant tumors of the rectum and colon, and common anorectal diseases.

Jian-Jin Xie Graduated with a bachelor's degree from Wenzhou Medical College in 2004. Since 2004, he has been working at Wenling City First People's Hospital, focusing on challenging anorectal conditions and common diseases.

Xia Li Graduated with a master's degree from Wenzhou Medical University in 2010. She has been working in the Colorectal Surgery Department at Wenling City First People's Hospital since 2010. Her research direction includes common anorectal diseases and challenging conditions.

ORCID

Xia Li  <http://orcid.org/0000-0002-5868-8907>

Authors' contribution

Xiao-Wei Wang, Ying-Hao Jiang and Wei Ye wrote the paper; Chun-Fa Shao, Jian-Jin Xie and Xia Li conceived the experiments; Xiao-Wei Wang and Ying-Hao Jiang analyzed the data; Wei Ye, Chun-Fa Shao and Xia Li collected and provided the sample for this study. All authors have read and approved the final submitted manuscript.

Ethics approval and consent to participate

Our work was performed with the approval of the Academic Ethics Committee of The First People's Hospital of Wenling and performed on the basis of the *Declaration of Helsinki*. All participants signed informed consent documentation. Animal experimentations were ratified by the Academic Ethics Committee of The First People's Hospital of Wenling and implemented on the basis of the Animal Welfare Legislation in China and ARRIVE Guidelines.

Availability of data and materials

The datasets used and/or analyzed during the current study are available from the corresponding author on reasonable request.

References

- Marmol I, Sanchez-de-Diego C, Pradilla Dieste A, Cerrada E, Rodriguez Yoldi MJ. Colorectal carcinoma: a general overview and future perspectives in colorectal cancer. *Int J Mol Sci.* 2017;18(1):197. PMID: 28106826. doi:10.3390/ijms18010197.
- Sagaert X, Vanstapel A, Verbeek S. 2018. Tumor heterogeneity in colorectal cancer: what do we know so far? *Pathobiology.* 85(1–2):72–84. doi: 10.1159/000486721. PMID: 29414818.
- Nojadedh JN, Behrouz Sharif S, Sakhinia E. Microsatellite instability in colorectal cancer. *Excli J.* 2018;17:159–168. doi:10.17179/excli2017-948. PMID: 29743854.
- Afshar S, Sedighi Pashaki A, Najafi R, Nikzad S, Amini R, Shabab N, Khiabanchian O, Tanzadehpanah H, Saidijam M. 2020. Cross-resistance of acquired radioresistant colorectal cancer cell line to gefitinib and regorafenib. *Iran J Med Sci.* 45(1):50–58. doi: 10.30476/ijms.2019.44972. PMID: 32038059.
- Bose D, Zimmerman LJ, Pierobon M, Petricoin E, Tozzi F, Parikh A, Fan F, Dallas N, Xia L, Gaur P, et al. Chemoresistant colorectal cancer cells and cancer stem cells mediate growth and survival of bystander cells. *Br J Cancer.* 2011;105(11):1759–1767. doi:10.1038/bjc.2011.449. PMID: 22045189
- Hsu HC, Liu YS, Tseng KC, Hsu CL, Liang Y, Yang TS, Chen JS, Tang RP, Chen SJ, Chen HC. 2013. Overexpression of Lgr5 correlates with resistance to 5-FU-based chemotherapy in colorectal cancer. *Int J Colorectal Dis.* 28(11):1535–1546. doi: 10.1007/s00384-013-1721-x. PMID: 23784051.
- Lee YH, Song NY, Suh J, Kim DH, Kim W, Ann J, Lee J, Baek JH, Na HK, Surh YJ. Curcumin suppresses oncogenicity of human colon cancer cells by covalently modifying the cysteine 67 residue of SIRT1. *Cancer Lett.* 2018;431:219–229. doi:10.1016/j.canlet.2018.05.036. PMID: 29807115.
- Cheng F, Su L, Yao C, Liu L, Shen J, Liu C, Chen X, Luo Y, Jiang L, Shan J, et al. SIRT1 promotes epithelial-mesenchymal transition and metastasis in colorectal cancer by regulating Fra-1 expression. *Cancer Lett.* 2016;375(2):274–283. doi:10.1016/j.canlet.2016.03.010. PMID: 26975631
- Yu DF, Jiang SJ, Pan ZP, Cheng WD, Zhang WJ, Yao XK, Li YC, Lun YZ. Expression and clinical significance of Sirt1 in colorectal cancer. *Oncol Lett.* 2016;11(2):1167–1172. PMID: 26893713. doi:10.3892/ol.2015.3982.
- Liu W, Zhang L, Xuan K, Hu C, Li L, Zhang Y, Jin F, Jin Y. Alkaline phosphatase controls lineage switching of mesenchymal stem cells by regulating the LRP6/GSK3beta complex in hypophosphatasia. *Theranostics.* 2018;8(20):5575–5592. PMID: 30555565. doi:10.7150/thno.27372.
- Wang M, Han D, Yuan Z, Hu H, Zhao Z, Yang R, Jin Y, Zou C, Chen Y, Wang G, et al. Long non-coding RNA H19 confers 5-Fu resistance in colorectal cancer by promoting SIRT1-mediated autophagy. *Cell Death Disease.* 2018;9(12):1149. doi:10.1038/s41419-018-1187-4. PMID: 30451820
- Zhao X, Wu Y, Li J, Li D, Jin Y, Zhu P, Liu Y, Zhuang Y, Yu S, Cao W, et al. JNK activation-mediated nuclear SIRT1 protein suppression contributes to silica nanoparticle-induced pulmonary damage via p53 acetylation and cytoplasmic localisation. *Toxicology.* 2019;423:42–53. doi:10.1016/j.tox.2019.05.003. PMID: 31082419.
- Pan JH, Zhou H, Zhu SB, Huang JL, Zhao XX, Ding H, Qin L, Pan YL. Nicotinamide phosphoribosyl transferase regulates cell growth via the Sirt1/P53 signaling pathway and is a prognosis marker in colorectal cancer. *J Cell Physiol.* 2019;234(4):4385–4395. PMID: 30191976. doi:10.1002/jcp.27228.
- Fujiwara Y, Saito M, Robles AI, Nishida M, Takeshita F, Watanabe M, Ochiya T, Yokota J, Kohno T, Harris CC, et al. A nucleolar stress-specific p53-mir-101 Molecular Circuit Functions as an Intrinsic Tumor-Suppressor Network. *EBioMedicine.* 2018; 33:33–48. doi:10.1016/j.ebiom.2018.06.031. PMID: 30049386.
- Moridikia A, Mirzaei H, Sahebkar A, Salimian J. MicroRNAs: Potential candidates for diagnosis and treatment of colorectal

- cancer. *J Cell Physiol.* **2018**;233(2):901–913. PMID: 28092102. doi:10.1002/jcp.25801.
16. Jiang M, Xu B, Li X, Shang Y, Chu Y, Wang W, Chen D, Wu N, Hu S, Zhang S, et al. O-GlcNacetylation promotes colorectal cancer metastasis via the miR-101-O-GlcNAc/EZH2 regulatory feedback circuit. *Oncogene.* **2019**;38(3):301–316. doi:10.1038/s41388-018-0435-5. PMID: 30093632
 17. Baker SA, Lombardi LM, Zoghbi HY. Karyopherin alpha 3 and karyopherin alpha 4 proteins mediate the nuclear import of methyl-CpG binding protein 2. *J Biol Chem.* **2015**;290(37):22485–22493. doi:10.1074/jbc.M115.658104. PMID: 26245896.
 18. Morris CP, Baune BT, Domschke K, Arolt V, Swagell CD, Hughes IP, Lawford BR, Mc DYR, Voisey J. KPNA3 variation is associated with schizophrenia, major depression, opiate dependence and alcohol dependence. *Dis Markers.* **2012**;33(4):163–170. doi:10.1155/2012/651707. PMID: 22960338.
 19. Liu T, Han Z, Li H, Zhu Y, Sun Z, Zhu A. **2018**. LncRNA DLEU1 contributes to colorectal cancer progression via activation of KPNA3. *Mol Cancer.* **17**(1):118. doi: 10.1186/s12943-018-0873-2. PMID: 30098595.
 20. He S, Shen J, Hu N, Xu X, Li J. DKK4 enhances resistance to chemotherapeutics 5-Fu and YN968D1 in colorectal cancer cells. *Oncol Lett.* **2017**;13(2):587–592. doi:10.3892/ol.2016.5461. PMID: 28356933.
 21. Qiao PF, Yao L, Zeng ZL. Catalpolmediated microRna34a suppresses autophagy and malignancy by regulating SIRT1 in colorectal cancer. *Oncol Rep.* **2020**;43(4):1053–1066. doi:10.3892/or.2020.7494. PMID: 32323786.
 22. Schee K, Boye K, Abrahamsen TW, Fodstad O, Flatmark K. Clinical relevance of microRNA miR-21, miR-31, miR-92a, miR-101, miR-106a and miR-145 in colorectal cancer. *Bmc Cancer.* **2012**;12(1):505. doi:10.1186/1471-2407-12-505. PMID: 23121918.
 23. Strillacci A, Valerii MC, Sansone P, Caggiano C, Sgromo A, Vittori L, Fiorentino M, Poggioli G, Rizzello F, Campieri M, et al. Loss of miR-101 expression promotes Wnt/beta-catenin signalling pathway activation and malignancy in colon cancer cells. *J Pathol.* **2013**;229(3):379–389. doi:10.1002/path.4097. PMID: 22930392
 24. Guo J, Ding Y, Yang H, Guo H, Zhou X, Chen X. RETRACTED: Aberrant expression of lncRNA MALAT1 modulates radioresistance in colorectal cancer in vitro via miR-101-3p sponging. *Exp Mol Pathol.* **2020**;115:104448. doi:10.1016/j.yexmp.2020.104448. PMID: 32380053.
 25. Ali Syeda Z, Langden SSS, Munkhzul C, Lee M, Song SJ. Regulatory mechanism of MicroRNA expression in cancer. *Int J Mol Sci.* **2020**;21(5). doi:10.3390/ijms21051723. PMID: 32138313.
 26. Chan SH, Wang LH. Regulation of cancer metastasis by microRNAs. *J Biomed Sci.* **2015**;22(1):9. PMID: 25614041. doi:10.1186/s12929-015-0113-7.
 27. Hur K, Toiyama Y, Takahashi M, Balaguer F, Nagasaka T, Koike J, Hemmi H, Koi M, Boland CR, Goel A. **2013**. MicroRNA-200c modulates epithelial-to-mesenchymal transition (EMT) in human colorectal cancer metastasis. *Gut.* **62**(9):1315–1326. doi: 10.1136/gutjnl-2011-301846. PMID: 22735571.
 28. de la Cruz-Morcillo MA, Valero ML, Callejas-Valera JL, Arias-Gonzalez L, Melgar-Rojas P, Galan-Moya EM, Garcia-Gil E, Garcia-Cano J, Sanchez-Prieto R, de la Cruz-Morcillo MA. P38MAPK is a major determinant of the balance between apoptosis and autophagy triggered by 5-fluorouracil: implication in resistance. *Oncogene.* **2012**;31(9):1073–1085. PMID: 21841826. doi:10.1038/onc.2011.321.
 29. Zhang C, Feng Y, Qu S, Wei X, Zhu H, Luo Q, Liu M, Chen G, Xiao X. Resveratrol attenuates doxorubicin-induced cardiomyocyte apoptosis in mice through SIRT1-mediated deacetylation of p53. *Cardiovasc Res.* **2011**;90(3):538–545. PMID: 21278141. doi:10.1093/cvr/cvr022.
 30. Schiffmann L, Eiken AK, Gock M, Klar E. Is the lymph node ratio superior to the Union for International Cancer Control (UICC) TNM system in prognosis of colon cancer? *World J Surg Oncol.* **2013**;11(1):79. PMID: 23521843. doi:10.1186/1477-7819-11-79.
 31. Torres A, Erices JI, Sanchez F, Ehrenfeld P, Turchi L, Virolle T, Uribe D, Niechi I, Spichiger C, Rocha JD, et al. Extracellular adenosine promotes cell migration/invasion of glioblastoma stem-like cells through A3 adenosine receptor activation under hypoxia. *Cancer Lett.* **2019**;446:112–122. doi:10.1016/j.canlet.2019.01.004. PMID: 30660649.